www.czasopisma.pan.pl PAN www.journals.pan.pl

ARCHIVES of FOUNDRY ENGINEERING

ISSN (2299-2944)
Volume 2025
Issue 1/2025

138 – 143

16/1

10.24425/afe.2025.153783

Published quarterly as the organ of the Foundry Commission of the Polish Academy of Sciences

Fading of Inoculation Effect in Grey Cast Iron

R. Jelínek, P. Bořil *, M. Kaněra, J. Doubrava, A. Záděra
Brno University of Technology, Czech Republic
* Corresponding author: E-mail address: 145312@vutbr.cz

Received 29.07.2024; accepted in revised form 07.01.2025; available online 17.03.2025

Abstract

The paper deals with the issue of inoculation of cast iron with flake graphite. In this paper, two different inoculants were chosen for the inoculation of cast iron with flake graphite and then compared. The first inoculant was the basic inoculant Alinoc, the second inoculant chosen was SB 5, which contains rare earth metals. One of the factors affecting the resulting quality of the structure and the occurrence of undesirable forms of graphite is the fading of the inoculation effect. This is due to the time delay between the time of inoculation and the casting of the metal. In this work, the graphitization effect as a function of the decay time was investigated for two different inoculants. After inoculation, samples were collected at time intervals for chill test piece, thermal analysis and chemical composition analysis using an optical spectrometer. The cast samples were subsequently subjected to metallographic evaluation of the microstructure and its quantification by image analysis of graphite.

Keywords: Inoculation, Inoculant, Grey cast iron, Thermal analysis, Image analysis

1. Introduction

Inoculation has been known since the 1930s and many different theories have been developed over the years to explain how inoculation works. Inoculation is widely used in foundries to improve the properties of cast iron and inoculation process uses a typical addition of between 0.05% to 1% of a specialized FeSi alloy containing controlled amounts of one or more elements, including Al, Ca, Ba, Sr, Ce, La, Mn, Bi, S, O, and Zr. The choice of element in the inoculant can affect the number of nuclei as well as the resulting mechanical properties of the cast iron [1, 2, 3].

By choosing a suitable inoculant, the formation of degenerate forms of graphite can be reduced or prevented. The high content of Si and Ni, especially in high silicon and niresist cast irons, has an effect on the appearance of graphite chunks, to prevent the formation of graphite chunks it is advisable to use inoculants without REM (rare earth metals) and to ensure a sufficient cooling rate of the casting. The inoculation leads to a decrease in the chill depth, depresses the formation of the D type graphite to form A type graphite and increases the eutectic cell number [4, 5].

The functionality of the inoculation effect of inoculants in cast iron can be determined by operational or laboratory tests. Thermal analysis provides high quality detailed information into the dynamic changes occurring upon melting and treatment of molten cast iron. The cooling curve, and its derivatives, displays patterns that can be used to predict the characteristics of a cast iron. This technique is used for understanding the solidification changes induced by compositional variation, solidification cooling rate and molten iron treatments, especially nodulizing and inoculation [6]. Thermal analysis methodology can be very successfully used to optimize and control the complicated cast iron solidification processes. The thermal analysis methodology has a good efficiency compared with other types of analysis (HB tests, structure analysis and chill tendency [7].

2. Experiment procedure

The aim of the experiment was to verify and compare the fading of two different inoculants as a function of time. The inoculants chosen for this experiment were Alinoc and SB 5, which are usually used for gray iron. First inoculant is basic inoculant which is expected to have a higher rate of fading. Second inoculant contains alkali earth metal and it is expected to have longer inoculation effect. The inoculation effect was assessed by chill test piece, thermal analysis and chemical analysis of the cast iron. Subsequently the metallographic analysis was performed, and evaluated by image analysis. Based on these results the rate of fading of these two inoculants. The effect of the inoculants on chill depth and on the structure of the samples was also determined.

2.1. Experiment description

First the charge was melted in Consarc crucible induction furnace with neutral ramming mass to prevent chemical contamination of the melt. The chemical composition was chosen to match the quality of EN GJL-200 cast iron for all melts. The granular inoculants (Alinoc and SB5) were chosen and added to the melt stream. Every five minutes the samples to determine the chemical composition, chill depth and thermal analysis were taken. After the castings have cooled down the chill test piece by breaking all the samples, which were casted to ISO-compliant mould. Analysis of the chemical composition of the samples was carried out on a Spark-Optical Emission Spectrometry TASMAN Q4. Carbon was determined using a G4 ICARUS CS combustion analyser. Thermal analysis data were continuously evaluated using Novacast's ATAS MetStar software, where only recalescence and liquid temperature values were evaluated. From the solidified samples for thermal analysis, cut-outs for image analysis were cut using a Struers Labotom 3 metallographic disrupter, which were subsequently pressed into the potting compound using an Ecopress 100 device from Metkon. The samples were ground and then polished to 1 µm. Finally, image analysis was performed using images from an Olympus DSX510 3D opto-digital microscope and post-processing was performed using Evident Corporation's PRECiV image analysis software.

Liquid metal preparation

For the purpose of the experiment, 2 melts were prepared with a charge weight of approx. 60 kg and marked 873 and 874. The metal was melted and then kept at a temperature range of 1394 °C to 1426 °C. For both melts a sample was taken to determine the chemical composition and the melts were alloyed to approximately the same chemical composition see Table 1 and Table 2.

Table 1.
Composition of melt 873 (after alloying, before inoculation)

C [%]	Si [%]	Mn [%]	P [%]	S [%]	Cr [%]	Mo [%]
3,05	1,54	0,72	0,05	0,06	0,07	0,01
Ni [%]	**Cu [%]**	**Al [%]**	**Co [%]**	**Ti [%]**	**V [%]**	**Fe [%]**
0,07	0,1	<0,0010	0,007	0,01	0,006	94,2

Table 2.
Composition of melt 874 (after alloying, before inoculation)

C [%]	Si [%]	Mn [%]	P [%]	S [%]	Cr [%]	Mo [%]
3,02	1,61	0,73	0,05	0,08	0,08	0,01
Ni [%]	**Cu [%]**	**Al [%]**	**Co [%]**	**Ti [%]**	**V [%]**	**Fe [%]**
0,05	0,1	<0,0010	0,007	0,01	0,004	94,2

2.2 The inoculation process

The inoculation process was the same for both inoculants. First, a portion of the molten metal was removed into a pan heated to approximately 1000 °C, and the inoculant was added to the stream as the melt was poured from the pan back into the furnace.

Melt 873 was inoculated with Alinoc basic inoculant with a grain size of 2-4 mm from Elkem, which is ferrosilicon-based and its inoculants contain calcium and aluminium (see Table 3 for composition). A total of 210 g of the inoculant was used in melt 873. This represents 0.35% of the weight of the charge, i.e. 0.35% of 60 kg.

Melt 874 was inoculated with SB5 with a grain size of 0.2 - 0.7 mm from ASK Chemicals. Similar to the Alinoc inoculant, it contains a ferrosilicon base, the crystallisation component consists of aluminium and calcium but additionally contains barium (see Table 3 for composition). A total of 210 g of inoculant was added to melt 874, i.e. 0.35% of the 60 kg charge.

Table 3.
Composition of inoculants used in the experiment [8]

	Composition				
Inoculant	**Si [%]**	**Al [%]**	**Ca [%]**	**Ba [%]**	**Fe [%]**
ALINOC	64 - 70	3,5 - 4,5	0,5 – 1,5	-	res.
SB5	65 - 73	1 – 1,5	0,8 – 1,5	2 - 3	res.

2.3 Preparation of samples to verify the fading effect of vaccines

A total of 9 samples were taken from each melt for the chill test piece evaluation and thermal analysis. The samples were labeled 873/0 to 873/8 and 874/0 to 874/8, with samples labeled 0 after the melt number taken before the actual inoculation and samples labeled 1 after the melt number taken immediately after the melt was inoculated. Subsequent samples were taken at five minute intervals each time. The last sample was taken 35 minutes after melt inoculation. Table 4 shows the change of carbon and silicon content, where the carbon loss can be observed during the experiment.

Table 4.
Carbon and silicon content after inoculation

sample / melting	1		8	
	% C	% Si	% C	% Si
873	2,99	1,77	2,87	1,79
874	3	1,86	2,86	1,85

The chill test piece

The principle of the turbidity test is to determine the graphitization ability of cast iron. A portion of the melt is cast into test mould with notch (see Figure 1). Two types of moulds are used. For the purpose of the experiment, the ISO test, which has a constant cross section, was used. The second method is by means of the so-called chill wedge test piece. In this type of test, the mould has a variable cross section and so cooling takes place at different rates. The constant cross-section mould is usually 85 mm high and is made of a core compound (croning). It is placed on a metal base, usually at least 30 mm thick, which guarantees increased heat dissipation. After solidification, we break this casting at the notch. In areas with the highest cooling rates, the solidification process results in the formation of a carbide structure (most commonly cementite Fe3C), which is referred to as chill. Chill reflects a certain sensitivity to cooling and also to crystallisation conditions. In general, chill forms at the point of rapid cooling. The lower the degree of eutecticity of the cast iron under given conditions, the faster the melt cools. The cooling rate is also higher for thin-walled castings and for castings with sharper outer edges and corners. Cast iron without free graphite is formed at the point of chill. At the point of slow temperature drop, the cast iron solidifies stably, forming a grey cast iron. At the transition point between the flake graphite and the chill, the mottled structure can be observed.

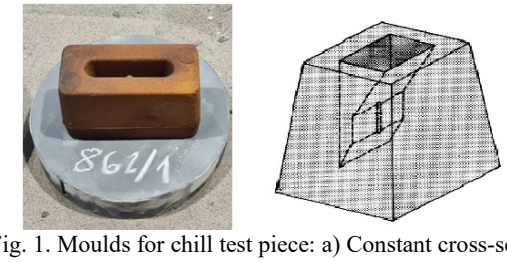

Fig. 1. Moulds for chill test piece: a) Constant cross-section mould (ISO test), b) Variable cross-section mould (wedge test piece) [9]

Thermal analysis

For the purpose of the experiment, crucibles ATAS G-cup without tellurium were chosen, which are suitable for the evaluation of the grey cast iron graphitization ability. The crucibles are placed on a special stand which transfers the thermoelectric voltage from the thermocouple to the A/D converter. The digital signal was further processed by NOVACAST's ATAS software. The approximate duration of the measurements was about 5 minutes, which corresponds to the solidification time in the crucible. [10, 11]

ATAS (Adaptive Thermal Analysis System), specifically ATAS MetStar, is a software from NOVACAST that is able to evaluate the digital signal during thermal analysis and process the data into cooling curves. Figure 2 shows the cooling curve with parameters and its first derivative.

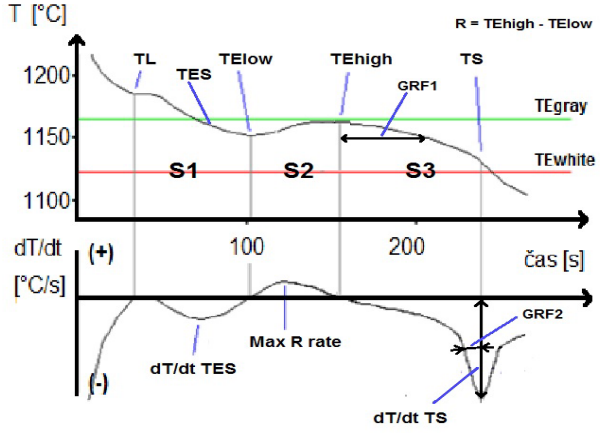

Fig. 2. ATAS cooling curve parameters including first derivative [10]

The parameters that ATAS works with are listed in Table 5. As mentioned above, it takes the program about five minutes to plot a curve, including the first derivative auxiliary curve. This represents the image of the actual solidification and the region it represents is the energy released in the crystallization process.

3 Results

3.1 Results of the chill test piece and thermal analysis

Figure 3 shows the chill level, i.e. the proportion of white cast iron formed, in the individual samples taken from melt 873. The smallest chill is found in sample 873/1, i.e. the sample taken immediately after inoculation with Alinoc inoculant. Subsequently, the sample taken at the fifth and tenth minute shows a gradual increase in chill level. It could be assumed that the inoculant gradually loses its effectiveness, but in sample 873/4, i.e. the sample taken at the fifteenth minute, there is again a slight decrease in chill level, which remains more or less the same until the thirtieth minute after inoculation.

Table 5.
ATAS parameters and their effect on their values during inoculation. [10]

Main parameters	Description	Desired effect of inoculation
TL	Liquidus temperature - the first time the temperature remains at the same value and austenite begins to be precipitated into the melt. For eutectic composition, TL=TElow.	Decrease
TElow	Minimum eutectic temperature - from this point the temperature increases to TEhigh; the first derivative is zero. The eutectic nucleation temperature.	Increase
TEhigh	Maximum eutectic temperature - after this value the temperature drops again. Solidification at high cooling rates may not reach this value; the first derivative is zero. Eutectic growth temperature.	Increase
TES	Solidification onset temperature of eutectic, not found in eutectic cast irons.	Increase
TS	Solidification temperature - the temperature at which the entire melt volume is solidified	Increase
GRF1	The first graphitization factor - indicates the time it takes for the temperature to drop from the TEhigh value by 15°C. During this time graphite crystallizes in the melt. A high value indicates a high amount of graphite has been excluded.	Increase
GRF2	The second graphitization factor - the angle on the first derivative curve in the TS solid region. A low value of the angle corresponds to a high thermal conductivity and is a sign of a high amount of excluded graphite.	Decrease
dT/dt TS	The first derivative on the TS solidus temperature.	Decrease
R	Recalescence - temperature difference between TEhigh and TElow. The optimum value is between 2-5°C.	Decrease

Thus, it can be concluded that the Alinoc inoculant, on the basis of the chill test piece performed, is able to work effectively for thirty minutes after inoculation of the cast iron. During this time the chill size was approximately the same and minor differences in chill size can be neglected. However, between 30 and 35 minutes there was a fading of the inoculating effect, which begins to decrease intensely after 35 minutes. At the end of the measurements, the determined chill level is comparable to that before inoculation.

Figure 3 shows the value of recalescence as a function of the depth of chill for melt 873. It is evident that the recalescence corresponds to the depth of chill. The initial value of recalescence for sample 873/0 was 8.6°C. After inoculation, both the chill and the recalescence value decreased to 6.3°C. This value was also the lowest value measured. Subsequently, the recalescence value stabilized between 6.5 and 7.5°C. For sample 873/7, the recalescence has already increased, although the depth of the chill has not changed and, from the point of view of the thermal analysis, it can already be said that the inoculation effect is fading. At 35 minutes, a recalescence value of 8.7°C was recorded, thus comparable to the initial value, i.e. before inoculation.

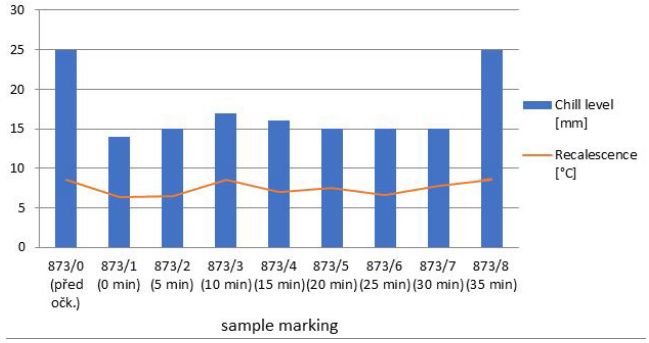

Fig. 3. Chill level of the samples compared to the recalescence value for melt 873

From Figure 4, it can be seen that the SB5 vaccine is most effective only around the fifth minute after the addition of the vaccine, which resulted in the shortest chill depth for sample 874/2 of all measured samples. Unfortunately, this trend did not last long and subsequently the chill depth increased and remained approximately the same. Between 30 and 35 minutes, the inoculating effect fades away and the original pre-inoculation chill level is slowly reached.

The inoculation effect for SB5 inoculant worked for thirty minutes. Subsequently, the inoculation effect faded away. It can be seen that after 35 minutes, the SB5 inoculant still shows a lesser depth of chill than before inoculation, but the fading effect is more than evident.

As the inoculation effect begins to fade, the recalescence value begins to rise. Thus, subcooling below the theoretical value (TELow) occurs, but because there are not as many nuclei in the melt, a few coarse nuclei grow, causing the temperature to rise (TEHigh) and heat is released. If there are few nuclei in the casting, the recalescence value is higher. However, the optimum condition is when the recalescence value is less during solidification. A small subcooling below the eutectic temperature

is sufficient to activate a larger number of nuclei on which graphite slowly grows, which is then finer.

Figure 4 shows that the recalescence value decreases from the initial 8.3°C to 5.2°C immediately after inoculation. For sample 874/2 there was also a slight increase and subsequently the recalescence ranged from 6.7 to 7.7°C. These values are therefore very similar to those of melt 873. In sample 874/7, a recalescence value of 8°C was already recorded, which indicates that the inoculating effect is already fading away, and in the sample taken at 35 minutes the recalescence was 8.9°C, a value higher than that of the sample taken before inoculation.

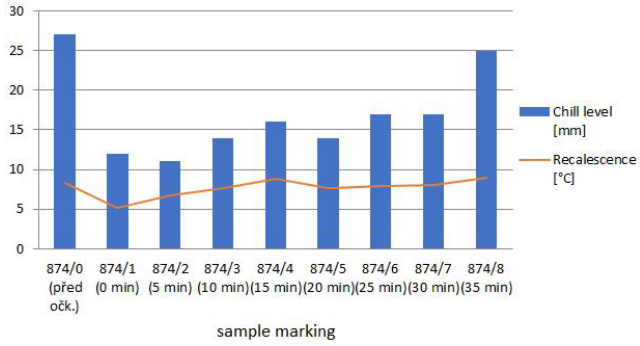

Fig. 4. Chill level of the samples compared to the recalescence value for melt 874

3.2 Image analysis

Immediately after inoculation with the Alinoc inoculant (sample 873/1), there is no change in the graphite structure and the sample is very similar to the sample taken before inoculation. In the following samples, there is a clear decrease in graphite size, which is also confirmed in Figure 5. The size of graphite in groups 5 and 6 decreases over time and the number of graphitic particles of size 8 increases. In the last sample (873/8) more than 65 % of the graphitic formations are smaller than 0.015 mm. An increase in dendritic structure is evident in the samples, which also corresponds to Figure 6.

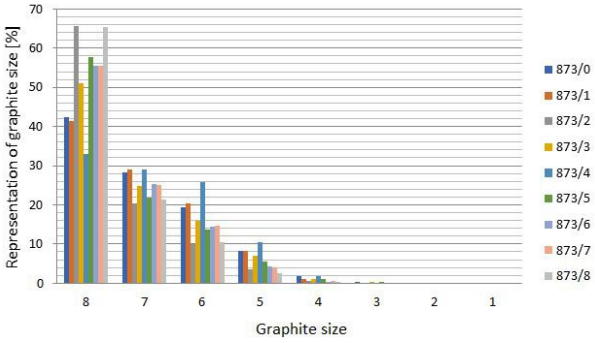

Fig. 5. Graphite size representation of individual melt samples 873

Thus, in sample 873/4, we observe the most uniform distribution in the structure, and subsequently there is a change to either a dendritically undirected or dendritically directed distribution of graphite. Unfortunately, interdendritically directed and interdendritically undirected (or rosette) graphite can occur in all samples. This is due to the lower concentration of carbon in the melt (strongly sub-eutectic cast iron), which still starts to decrease after grafting. From Figure 7 it is possible to assess the changes in graphite shape with time. The amount of flake graphite gradually decreases as the grafting effect fades. Smaller, more compact formations begin to appear and image analysis classifies them as spider or compacted graphite.

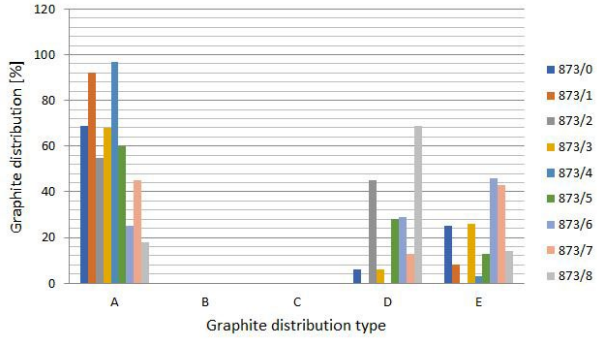

Fig. 6. Representation of graphite distribution type of individual melt samples 873.

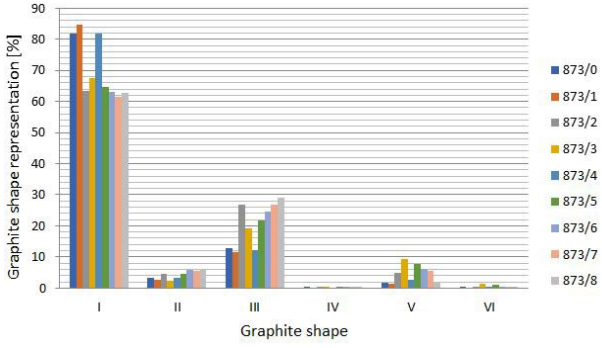

Fig. 7. Graphite shape representation of individual melt samples 873

Figure 8 shows the increase in graphite size after inoculation with SB5 compared to uninoculated cast iron.

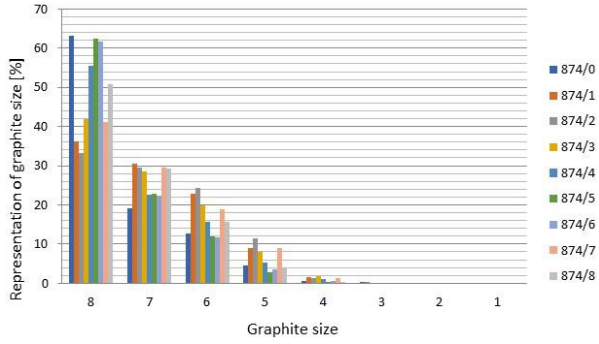

Fig. 8. Graphite size representation of individual melt samples 874

Between the tenth and fifteenth minute after inoculation, the representation of graphitic particles of size 8 increases again. In Figure 9, we can observe an increase of dendritic structure, where more than 90 percent of the graphite distribution is interdendritically directed in sample 874/8. In Figure 10, we can again observe the loss of flake graphite due to the fading of the inoculation effect.

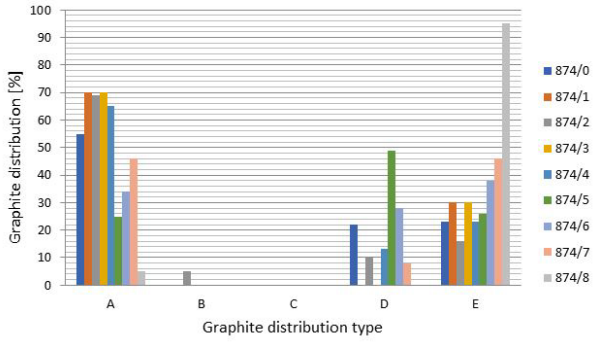

Fig. 9. Representation of graphite distribution type of individual melt samples 874

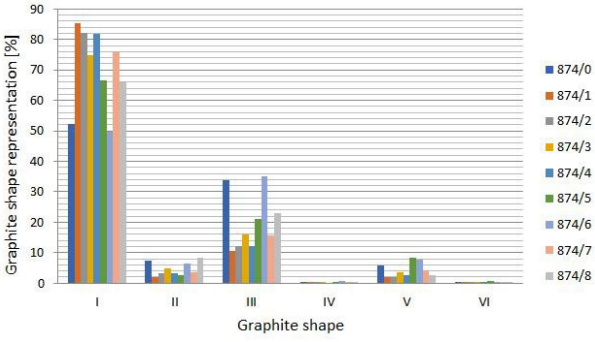

Fig. 10. Graphite shape representation of individual melt samples 874

4. Conclusions

Based on the evaluation of the recalescence data, it can be stated that both inoculants were effective for the same period of time.

For samples taken immediately after inoculation, the value was the lowest and subsequently the recalescence stabilised at similar values for both inoculants. Both inoculants worked safely for 25 minutes and a gradual fading of the inoculant effect was observed at 30 minutes.

Compared to the chill test pieces, thermal analysis detected that the usability of both inoculants is ideally five minutes shorter.

Image analysis also confirms the fading of the inoculating effect, mainly by an increasing proportion of interdendritically directed and undirected graphite at the expense of flake graphite.

The SB 5 inoculant has a better inoculation effect in the first 10 minutes, the duration of the vinoculation effect is comparable for both inoculants.

Acknowledgements

This work was supported by the specific research project of BUT FME Brno, no. FSI-S-22-8015 research on melting and metallurgical processing of high-temperature alloys.

References

[1] Hartung, C., Michels, L. & Logan, R. (2021). The evolution of inoculants. *Modern Casting*. 111(10), 24-29.

[2] Lia, B.-G., Sim, K.-H., & Kim, R.-C. (2019). Effect of Sb–Ba–Ce–Si–Fe post inoculants on microstructural and mechanical properties of As-cast pearlitic ductile iron. *Steel research international*. 90(5). https://doi.org/10.1002/srin.201800530.

[3] Dwulat, R., Janerka, K. & Grzesiak, K. (2021). The influence of final inoculation on the metallurgical quality of nodular cast iron. *Archives of Foundry Engineering*. 21(4), 5-14. https://doi.org/10.24425/afe.2021.138673.

[4] Mrvar, P., Mihalic Pokopec, I., Petrič, M. & Bauer, B. (2018). Effect of Si and Ni addition on graphite morphology in heavy-section spheroidal graphite iron parts. *Materials Science Forum*. 925, 70-77. https://doi.org/10.4028/www.scientific.net/MSF.925.70.

[5] Nakae, H. (2008). Influence of inoculation on solidification in cast iron. *International Journal of Cast Metals Research*. 21(1-4), 7-10. https://doi.org/10.1179/136404608X361576.

[6] Stan, S., Firican, C., Stefan, I. & Riposan, I. (2016). Thermal analysis to optimize and control the cast iron solidification process. *Solid State Phenomena*. 254, 14-19. https://doi.org/10.4028/www.scientific.net/SSP.254.14.

[7] Stefan, E. M. & Chisamera, M. (2015). Solidification control by thermal analysis of la/ba inoculated grey cast iron. *Advanced Materials Research*. 1128, 35-43. https://doi.org/10.4028/www.scientific.net/AMR.1128.35.

[8] Elkem Foundry Products. (2012). *Alinoc Inoculant. YUMPU*. Retrieved March 23, 2024, from https://www.yumpu.com/en/document/read/11944545/alinoc r-inoculant-elkem.

[9] Foundry Lexicon. (2024). *Chill wedge test piece*. Retrieved April 23, 2024, from https://www.giessereilexikon.com/en/foundry-lexicon/Encyclopedia/show/chill-wedge-test-piece-3794/?cHash=67a9441603ce8fc97526f4b623629871.

[10] Chyla, O. (2016). *Verification of the effect of inoculants on the structure of cast iron using thermal analysis*. Diploma thesis, Brno University of Technology, the Czech Republic (in Czech).

[11] NOVACAST. Controlling Metallurgy. Retrieved April 23, 2024, from https://www.novacast.se/product/